Electronic Supplementary Information

Vanadium complexes derived from oxacalixarenes: structural studies and use in the ring opening polymerization of ε-caprolactone and δ-valerolactone and ethylene polymerization

Tian Xing,[a] Timothy J. Prior,[a] Mark R. J. Elsegood,[b] Nina V. Semikolenova,[c] Igor E. Soshnikov,[c,d] Konstantin Bryliakov[c,d] Kai Chen[a,e] and Carl Redshaw[a]*

[a] *Plastics Collaboratory, Department of Chemistry, University of Hull, Cottingham Road, Hull, HU6 7RX, UK.*

[b] *Chemistry Department, Loughborough University, Loughborough, Leicestershire, LE11 3TU, UK.*

[c] *Boreskov Institute of Catalysis, Pr. Lavrentieva 5, Novosibirsk 630090, Russian Federation.*

[d] *Novosibirsk State University, Pirogova 1, Novosibirsk 630090, Russian Federation.*

[e] *Collaborative Innovation Center of Atmospheric Environment and Equipment Technology, Jiangsu Key Laboratory of Atmospheric Environment Monitoring and Pollution Control, School of Environmental Science and Engineering, Nanjing University of Information Science & Technology, Nanjing 210044, P. R. China.*

Crystallography

Figure S1. Molecular structures of (a) $[(VO)_4L^1]$ (**2**) (b) $[V(Np\text{-}(OMe)C_6H_4)]_2L^1$ (**4**) (hydrogens and four MeCN molecules are omitted for clarity), (c) $[V(Np\text{-}(CF_3)C_6H_4)]_2L^1$ (**5**), (d) $[V(Np\text{-}Cl\text{-}C_6H_4)]_2L^1$ (**6**).

ROP studies

Table S1. ROP of ε-CL using **1-8** and **I-IV** in the absence of BnOH.

Table S2. ROP of *δ*-VL using **1-8** and **I-IV** in the absence of BnOH.

Table S3. ROP of co-polymer (*ε*-CL +*δ*-VL) using **1 – 8** and **I – IV** in the absence of BnOH.

Figure S2. (a) Relationship between conversion and time for the polymerization of *ε*-CL by using complex **1-3**, **8**, and **I-IV**; (b) Relationship between conversion and time for the polymerization of *ε*-CL by using complexes **3-7**; Condition: T=130 °C, $n_{Monomer}$: n_V: BnOH=500 : 1: 0.

Figure S3. (a) Relationship between conversion and time for the polymerization of *δ*-VL by using complexes **1-3**, **8**, and **I – IV**; (b) Relationship between conversion and time for the polymerization of *δ*-VL by using complexes **3-7**; Condition: T=130 °C, $n_{Monomer}$: n_V: BnOH=500 : 1: 0.

Figure S4. (a) Relationship between conversion and time for the saturation kinetics polymerization of CL by using complex **1**/BnOH; Condition: T=130 °C, $n_{Monomer}$: n_V: BnOH=500: 1: 1.

Figure S5. Mass spectrum of PCL by using **6** in the absence of BnOH (run 10, Table S1).

Figure S6. Mass spectrum of PCL by using **5** with BnOH (run 10, Table 2). [M = n × 114.14 (CL) + 108.05 (BnOH) +22.99 (Na^+)].

Figure S7. Mass spectrum of PVL by using **7** in the absence of BnOH (run 11, Table S2).

Figure S8. Mass spectrum of PVL by using **7**/BnOH (run 12, Table 3). [M = 108.05 (BnOH) + n × 100.12 (VL) + 22.99 (Na^+)].

Figure S9. Mass spectrum of CL-VL Copolymer (1:1 ratio CL/VL) by using **I** in the absence of BnOH (run 14, Table 4).

Figure S10. ^{1}H NMR spectrum ($CDCl_3$, 400 MHz, 298 K) of the PCL synthesized with **6** in the absence of BnOH (run 10, Table S1).

Figure S11. ^{1}H NMR spectrum ($CDCl_3$, 400 MHz, 298 K) of the PCL synthesized with **6**/BnOH (run 11, Table 2).

Figure S12. ^{1}H NMR spectrum ($CDCl_3$, 400 MHz, 298 K) of the PVL synthesized with **8** in the absence of BnOH (run 12, Table S2).

Figure S13. ^{1}H NMR spectrum ($CDCl_3$, 400 MHz, 298 K) of the PVL synthesized with **1**/BnOH (run 1, Table 3).

Figure S14. ^{1}H NMR spectrum ($CDCl_3$, 400 MHz, 298 K) of the CL-VL Copolymer (1:1 ratio CL/VL) synthesized with **I** in the absence of BnOH. (run 15, Table 4).

Figure S15. ^{1}H NMR spectrum ($CDCl_3$, 400 MHz, 298 K) of the CL-VL Copolymer (1:1 ratio CL/VL) synthesized with **1**/BnOH. (run 2, Table 4).

Figure S16. ^{13}C NMR spectrum ($CDCl_3$, 400 MHz, 298 K) of the CL-VL Copolymer (65-63 ppm)

Equation S1. Determination of number-average sequence length for CL

Equation S2. Determination of number-average sequence length for VL.

Equation S3. Determination of the Randomness Character (R).

Complex characterization

Figure S17-S24. ^{1}H NMR ($CDCl_3$) results of complex **1-8**.

Polyethylene spectra

Figure S25 and S26. ^{1}H and ^{13}C NMR spectra ($Cl_2C_6H_4$, 100 °C) of polyethylene (run 6, Table 5).

Crystallography

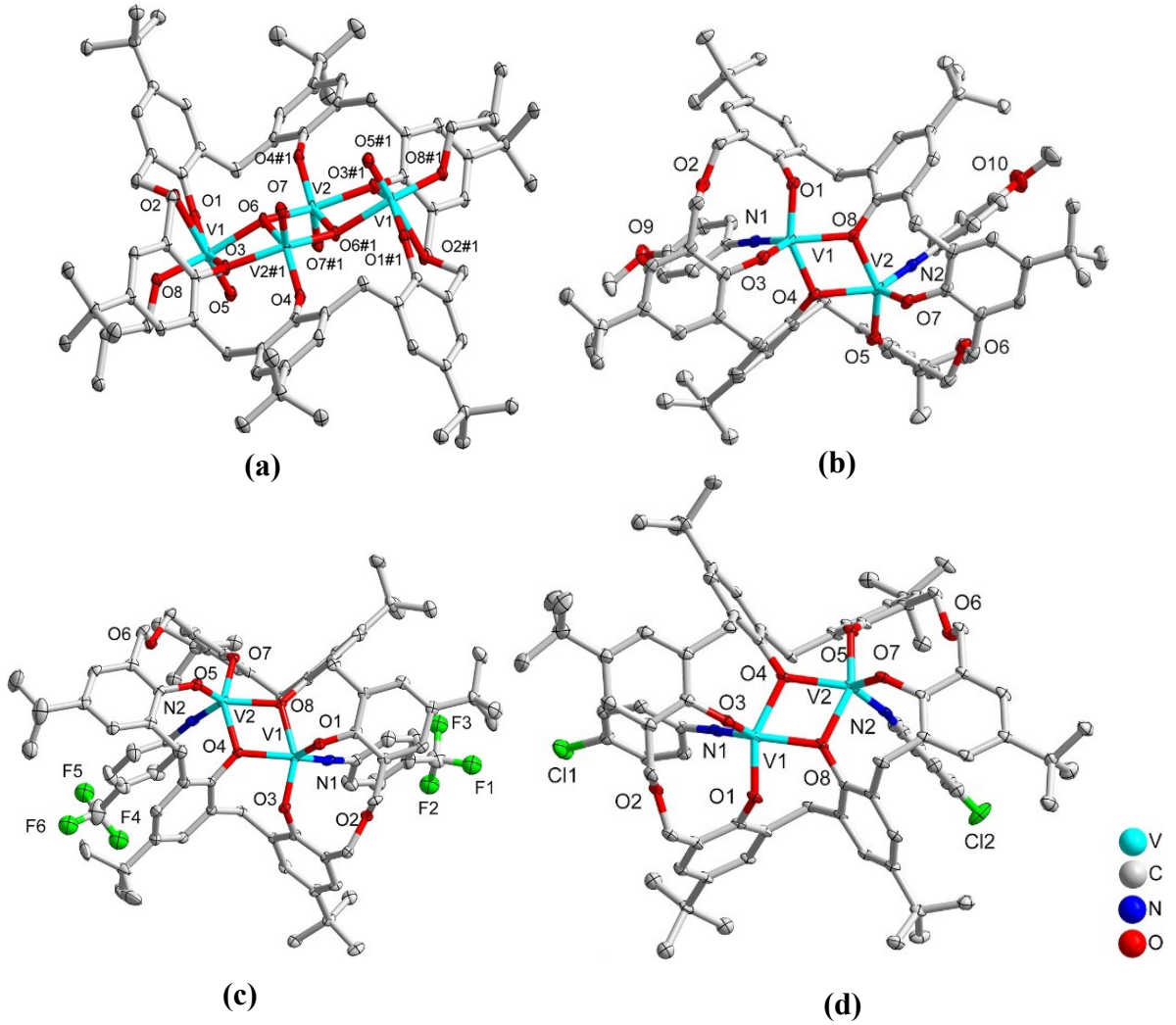

Figure S1. Molecular structures of (a) $[(VO)_4L^1]$ (**2**) (b) $[V(Np\text{-}(OMe)C_6H_4)]_2L^1$ (**4**) (hydrogens and four MeCN molecules are omitted for clarity), (c) $[V(Np\text{-}(CF_3)C_6H_4)]_2L^1$ (**5**), (d) $[V(Np\text{-}Cl\text{-}C_6H_4)]_2L^1$ (**6**).

Refinement details.

Single crystal X-ray diffraction for samples **1-6** were collected by the UK National Crystallography Service on various instruments. Samples were mounted at the end of MiTiGen loops and held at 100 K in an Oxford Cryosystems nitrogen gas cryostream. Data were collected in series of ω-scans, and were corrected for the effects of absorption using a multi-scan process.

Single crystal X-ray diffraction data for sample **8** were collected at Station 9.8 of the UK Synchrotron Radiation Source at Daresbury. The sample was mounted at the end of a two-stage glass fibre and held at 150 K using an Oxford Cryosystems nitrogen gas cryostream. Data were collected in series of ω-scans. Data were corrected for the effects of beam decay and absorption using SADABS. (Bruker (2001).

SADABS. Bruker AXS Inc., Madison, Wisconsin, USA.)

Each sample was solved using standard procedures within one version of SHELXS (direct methods, G. M. Sheldrick, *Acta Cryst*. 2008, **A64**, 112-122) or SHELXT (dual space methods, G. M. Sheldrick, *Acta Cryst.* 2015, A**71**, 3-8). Structures were refined against all observed F^2 values using SHELXL (G. M. Sheldrick, *Acta Cryst*. 2015, **C71**, 3-8).

Structure solution and refinement was routine. For the structures **1**, **2**, **3**, **5**, **6**, and **8** small-scale disorder modelled using standard techniques.

The crystal of **4** examined was found to be twinned. The two twin domains were related by a 180° rotation about the 0 0 1 reciprocal axis. Reflections from both components were integrated separately and all observed data used in the final refinement (SHELXL HKLF5 formalism). The two twin components were present in these amounts 0.8557: 0.1443(4). The data for refinement were trimmed at 0.8 Å resolution.

ROP studies

Table S1 ROP of ε-CL using **1** – **8** and **I - IV** in the absence of BnOH.

Run	Cat.	CL: V: BnOH	T/°C	t/h	Conv[a] (%)	$M_{n,GPC}\times10^{-3}$[b]	$M_w\times10^{-3}$[b]	$M_{n,Cal}\times10^{-}$	PDI[d]	TON[e]	TOF (h^{-1})[f]
1	**1**	1000:1:0	130	24	98.5	7.13	10.57	112.43	1.48	985	41
2	**1**	500:1:0	130	24	99.7	8.21	11.64	56.90	1.41	499	21
3	**1**	250:1:0	130	24	97.5	5.14	6.51	27.78	1.27	244	10
4	**1**	100:1:0	130	24	98.1	2.69	3.14	11.18	1.16	98	4
5	**1**	50:1:0	130	24	90.4	0.97	1.66	5.13	1.71	452	19
6	**2**	500:1:0	130	24	64.1	2.65	3.91	36.48	1.47	321	13
7	**3**	500:1:0	130	24	99.1	2.84	3.20	56.56	1.12	496	21
8	**4**	500:1:0	130	24	97.9	1.37	2.22	55.80	1.61	490	20
9	**5**	500:1:0	130	24	99.4	6.08	8.88	56.66	1.46	497	21
10	**6**	500:1:0	130	24	99.0	5.67	8.11	56.43	1.43	495	21
11	**7**	500:1:0	130	24	96.3	5.35	8.76	54.89	1.63	482	20
12	**8**	500:1:0	130	24	99.7	5.52	8.76	56.90	1.59	499	21
13	**8**	500:1:0	100	24	77.1	2.91	4.38	43.94	1.50	386	16
14	**8**	500:1:0	80	24	nothing	-	-	-	-	-	-
15	**I**	500:1:0	130	24	46.3	2.51	3.60	32.63	1.41	232	10
16	**II**	500:1:0	130	24	65.1	3.54	4.32	32.71	1.21	326	14
17	**III**	500:1:0	130	24	57.6	3.96	5.20	41.36	1.31	288	12
18	**IV**	500:1:0	130	24	60.3	2.27	3.78	38.61	1.66	302	13

[a] Determined by ^{1}H NMR spectroscopy. [b] $M_{n/w}$, GPC values corrected considering Mark–Houwink method from polystyrene standards in THF, $M_{n/w}$ measured = 0.56 × $M_{n/w}$ GPC ×10^3. [c] Calculated from ([monomer]$_0$/[cat]$_0$) × conv (%) × monomer molecular weight (M_{CL}=114.14). [d] From GPC. [e] Turnover number (TON) = number of moles of ε-CL consumed/ number of moles V. [f] Turnover frequency (TOF) = TON/time (h).

Table S2. ROP of *δ*-VL using **1** – **8** and **I - IV** in the absence of BnOH.

Run	Cat.	VL: V: BnOH	T/°C	t/h	Conv[a] (%)	$M_{n,GPC}\times10^{-3}$[b]	$M_w\times10^{-3}$[b]	$M_{n,Cal}\times10^{-3}$[c]	PDI[d]	TON[e]	TOF (h^{-1})[f]
1	**1**	1000:1:0	130	24	93.5	2.51	3.75	93.61	1.44	935	39
2	**1**	500:1:0	130	24	90.7	3.46	5.48	45.40	1.59	454	19
3	**1**	250:1:0	130	24	95.1	2.36	3.21	23.77	1.36	238	10
4	**1**	100:1:0	130	24	92.4	1.56	2.95	9.24	1.89	92	4
5	**1**	50:1:0	130	24	93.0	0.53	1.36	4.65	2.56	465	19
6	**2**	500:1:0	130	24	60.2	2.41	3.88	43.20	1.61	301	13
7	**3**	500:1:0	130	24	77.3	1.37	2.22	38.69	1.62	387	16
8	**4**	500:1:0	130	24	99.5	3.06	4.93	56.54	1.61	498	21
9	**5**	500:1:0	130	24	99.1	7.64	12.65	56.67	1.65	496	21
10	**6**	500:1:0	130	24	99.6	3.97	5.08	56.33	1.28	498	21
11	**7**	500:1:0	130	24	93.4	4.29	6.23	46.77	1.45	467	19
12	**8**	500:1:0	130	24	99.4	9.08	12.86	49.76	1.42	497	21
13	**8**	500:1:0	100	24	90.4	5.44	6.36	45.25	1.16	452	19
14	**8**	500:1:0	80	24	nothing	-	-	-	-	-	-
15	**I**	500:1:0	130	24	83.1	1.89	2.43	41.55	1.33	416	17
16	**II**	500:1:0	130	24	92.1	3.27	4.14	46.60	1.26	461	19
17	**III**	500:1:0	130	24	79.2	2.53	4.12	33.12	1.63	396	17
18	**IV**	500:1:0	130	24	86.2	3.55	5.67	41.23	1.60	431	18

[a] Determined by ^{1}H NMR spectroscopy. [b] $M_{n/w}$, GPC values corrected considering Mark–Houwink method from polystyrene standards in THF, $M_{n/w}$ measured = 0.57 × $M_{n/w}$ GPC ×10^3. [c] Calculated from ([monomer]$_0$/[cat]$_0$) × conv (%) × monomer molecular weight (M_{VL}=100.16). [d] From GPC. [e] Turnover number (TON) = number of moles of *δ*-VL consumed/ number of moles V. [f] Turnover frequency (TOF) = TON/time (h).

Table S3. ROP of co-polymer (*ε*-CL +*δ*-VL) using **1 – 8** and **I – IV** in the absence of BnOH**.**

Run	Cat	CL:VL:V:BnOH	T/°C	CL:VL[a]	Conv[b] (%)	$M_{n,GPC}\times10^{-3}$[c]	$M_w\times10^{-3}$[c]	PDI[d]
1	**1**[e]	250:250:1:0	130	46:54	64.3	8.53	11.38	1.33
3	**2**[e]	250:250:1:0	130	-	-	-	-	-
4	**3**[e]	250:250:1:0	130	35:65	37.5	3.45	5.67	1.64
5	**4**[e]	250:250:1:0	130	34:66	43.9	4.74	7.36	1.55
6	**5**[e]	250:250:1:0	130	40:60	55.1	6.88	9.71	1.41
7	**5**[f]	250:250:1:0	130	62:38	60.6	8.92	24.9	2.79
8	**5**[g]	250:250:1:0	130	58:42	30.5	3.65	5.46	1.49
9	**6**[e]	250:250:1:0	130	42:58	54.2	4.56	6.15	1.34
10	**6**[f]	250:250:1:0	130	66:34	52.3	6.84	8.79	1.28
11	**6**[g]	250:250:1:0	130	45:55	33.5	4.05	6.88	1.69
12	**7**[e]	250:250:1:0	130	40:60	55.9	4.36	6.75	1.54
13	**8**[e]	250:250:1:0	130	59:41	46.3	4.91	6.48	1.32
15	**I**[e]	250:250:1:0	130	41:59	60.1	6.67	10.45	1.58
16	**I**[e]	250:250:1:0	130	38:62	54.2	2.15	3.52	1.63
17	**II**[e]	250:250:1:0	130	36:64	58.3	3.93	5.65	1.43
18	**III**[e]	250:250:1:0	130	35:65	43.3	2.38	4.36	1.84
19	**IV**[e]	250:250:1:0	130	36:64	36.2	3.63	5.75	1.58

[a] Ratio of ε-CL to δ-VL observed in the co-polymer by ^{1}H NMR spectroscopy. [b] Determined by ^{1}H NMR spectroscopy. [c] $M_{n/w}$, GPC values corrected considering Mark–Houwink method from polystyrene standards in THF, $M_{n/w}$ measured = [0.56 × $M_{n/w}$ GPC × (1-%CL) + 0.57 × $M_{n/w}$ GPC ×(1-%VL)] × 10^3. [d] From GPC. [e] ε-Caprolactone was firstly added for 24 h, then δ-valerolactone was added and heating for 24 h. [f] δ-valerolactone was firstly added for 24 h, then ε-caprolactone was added and heating for 24 h. [g] ε-caprolactone and δ-valerolactone were added in the same time and heating for 24 h.

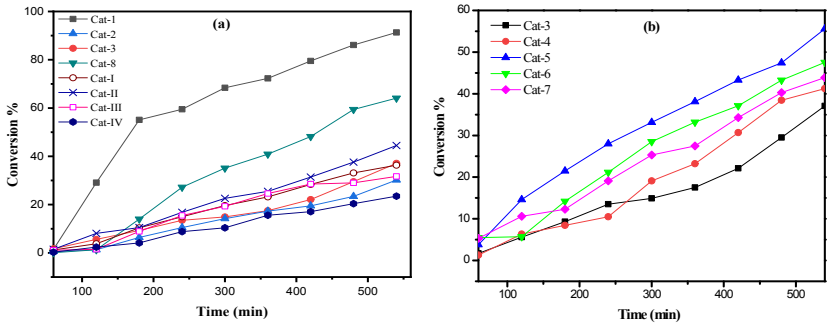

Figure S2. (a) Relationship between conversion and time for the polymerization of ε-CL by using complex **1-3**, **8**, and **I-IV**; (b) Relationship between conversion and time for the polymerization of ε-CL by using complexes **3-7**; Condition: T=130 °C, $n_{Monomer}$: n_V: BnOH=500 : 1: 0.

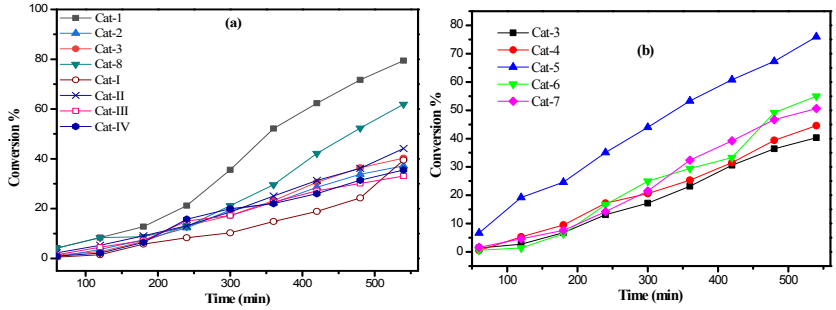

Figure S3. (a) Relationship between conversion and time for the polymerization of δ-VL by using complexes **1-3**, **8**, and **I – IV**; (b) Relationship between conversion and time for the polymerization of δ-VL by using complexes **3-7**; Condition: T=130 °C, $n_{Monomer}$: n_V: BnOH=500 : 1: 0.

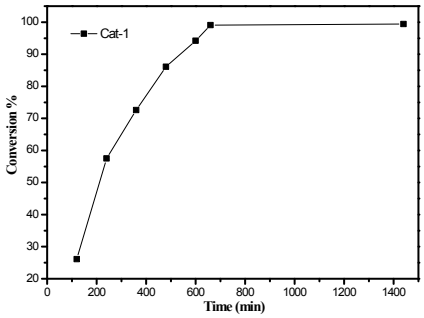

Figure S4. (a) Relationship between conversion and time for the saturation kinetics polymerization of CL by using complex **1**/BnOH; Condition: T=130 °C, $n_{Monomer}$: n_V: BnOH=500: 1: 1.

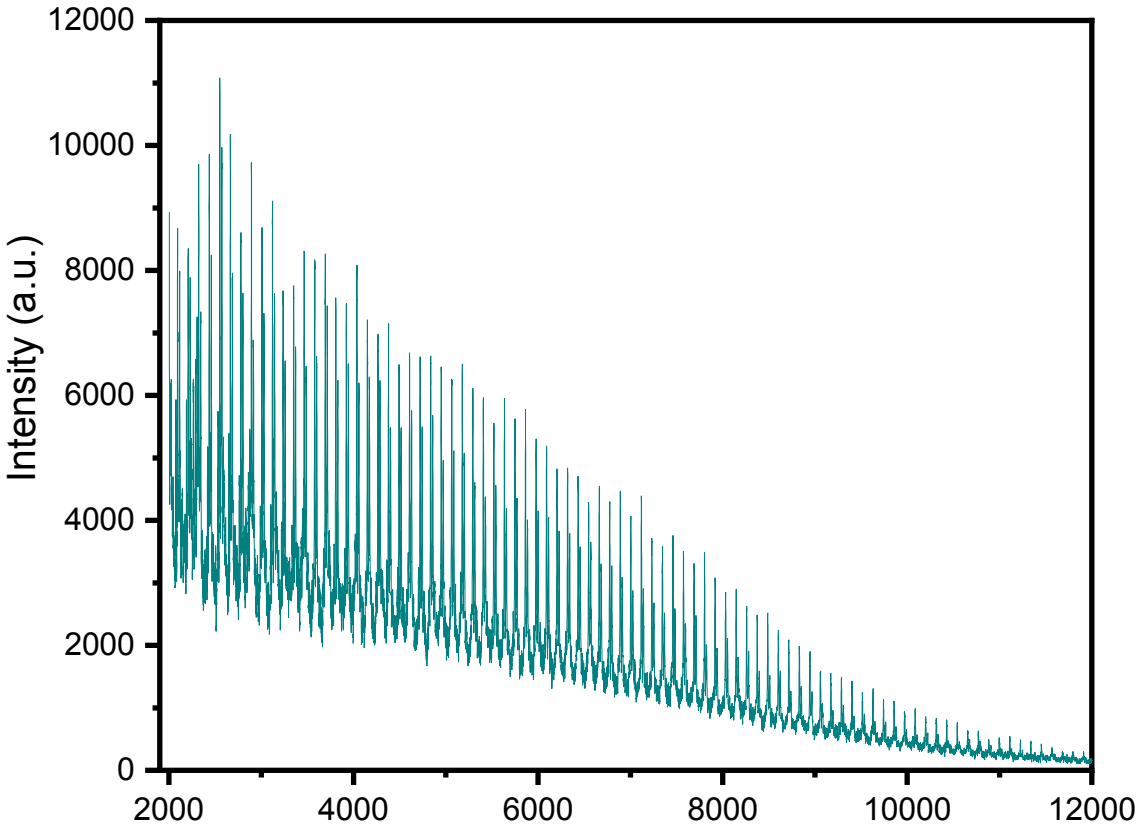
Intensity (a.u.)
12000
10000
8000
6000
4000
2000
0
2000
4000
6000
8000
10000
12000

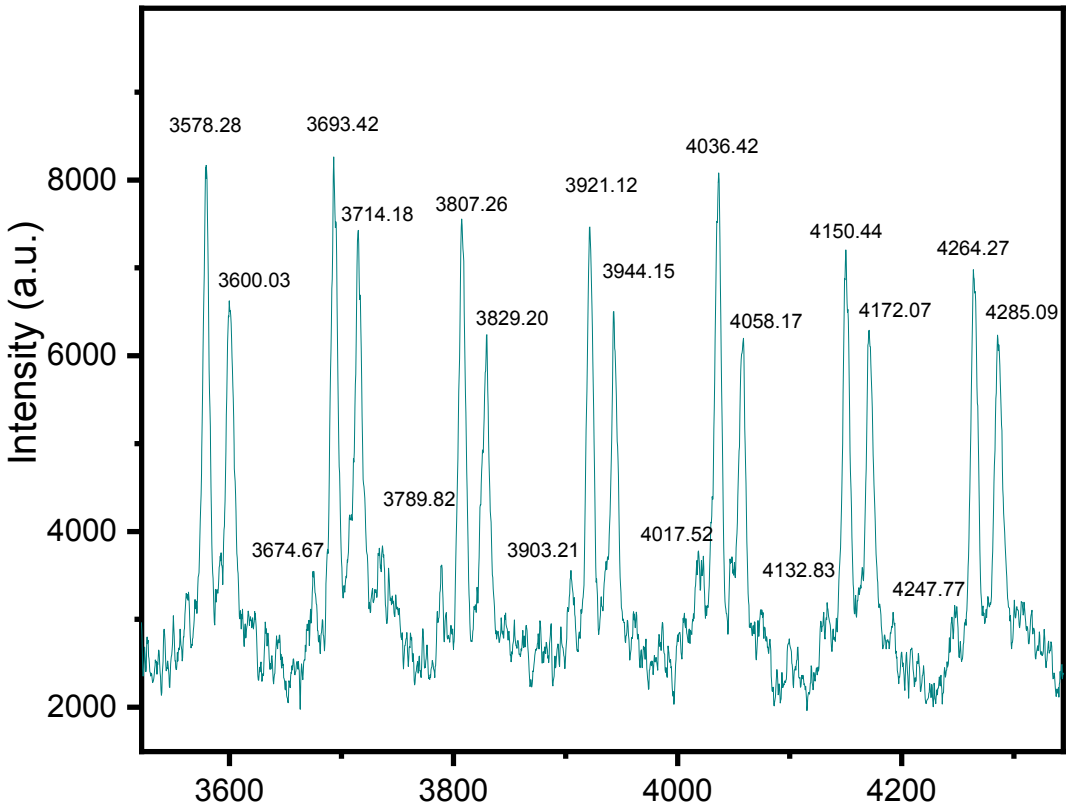
Intensity (a.u.)
8000
6000
4000
2000
3600
3800
4000
4200
3578.28
3693.42
4036.42
3921.12
3714.18
3807.26
4150.44
4264.27
3600.03
3944.15
4172.07
4285.09
3829.20
4058.17
3789.82
3674.67
3903.21
4017.52
4132.83
4247.77

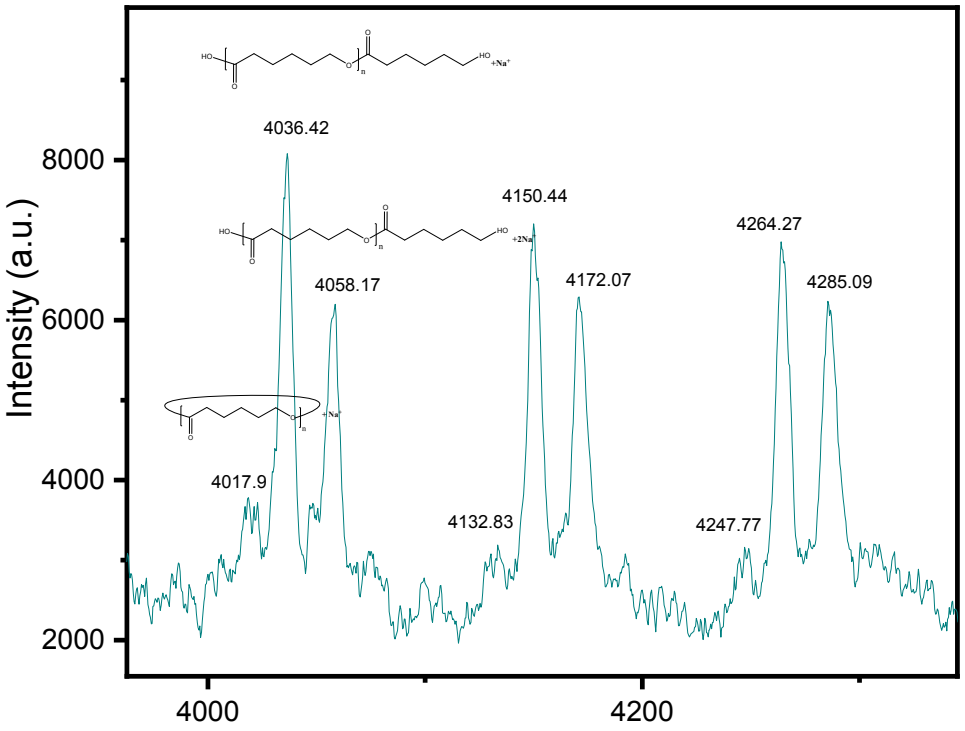

Figure S5. Mass spectrum of PCL by using **6** in the absence of BnOH (run 10, Table S1).

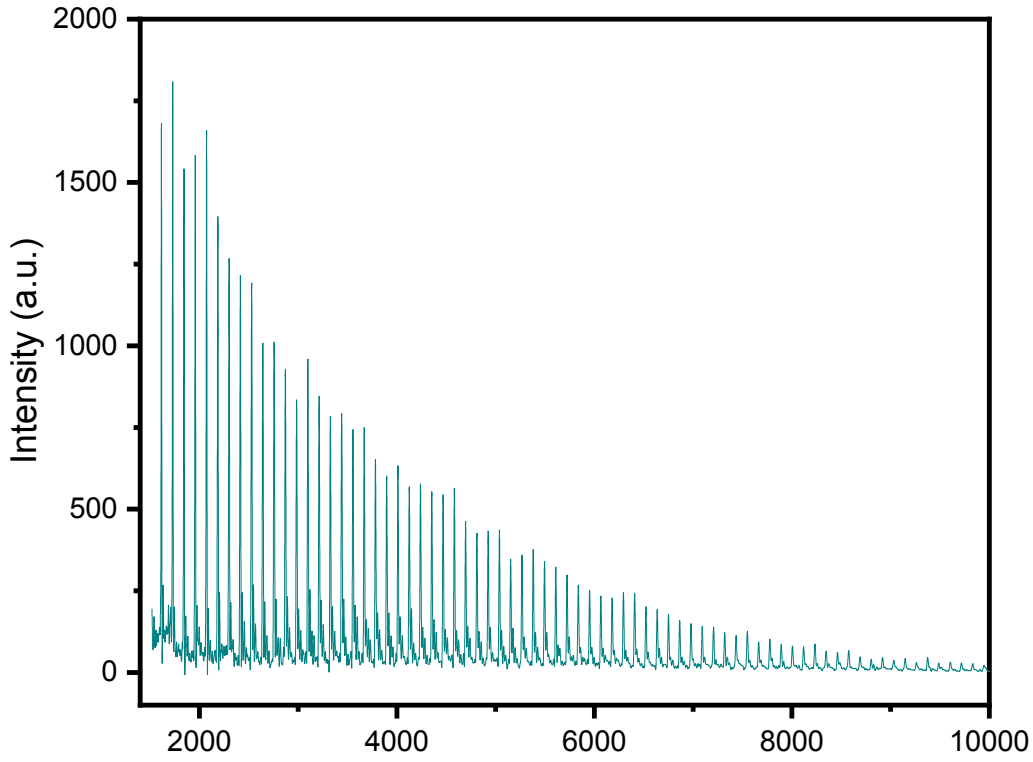

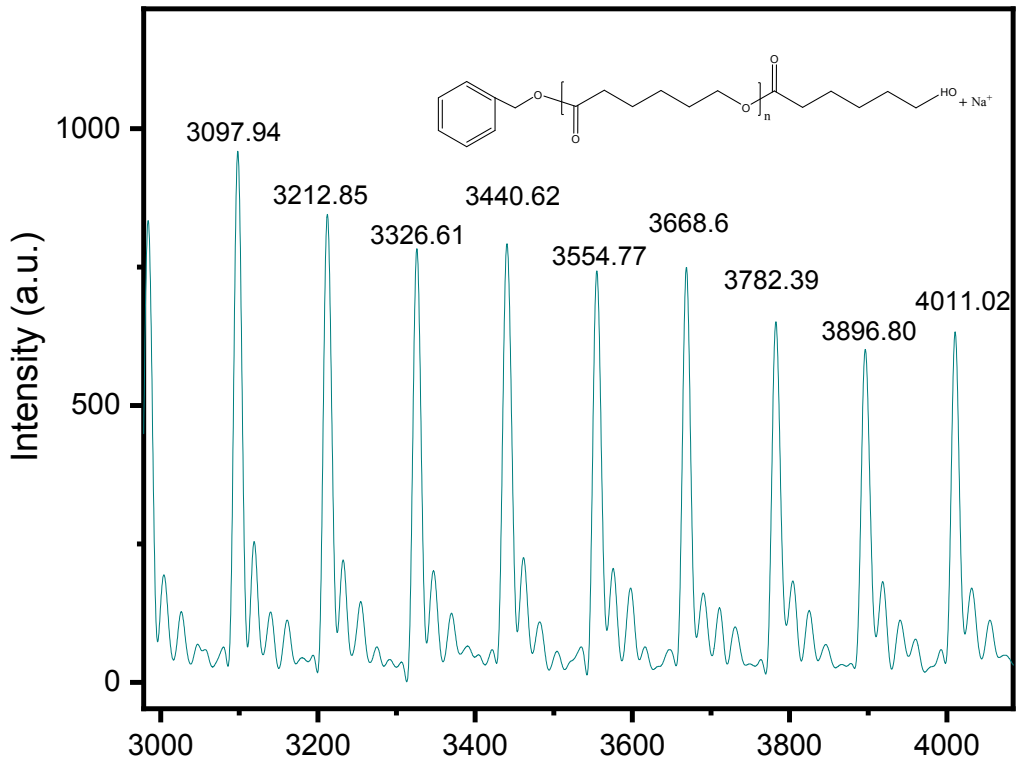

Figure S6. Mass spectrum of PCL by using **5** with BnOH (run 10, Table 2). [M = n × 114.14 (CL) + 108.05 (BnOH) +22.99 (Na^+)].

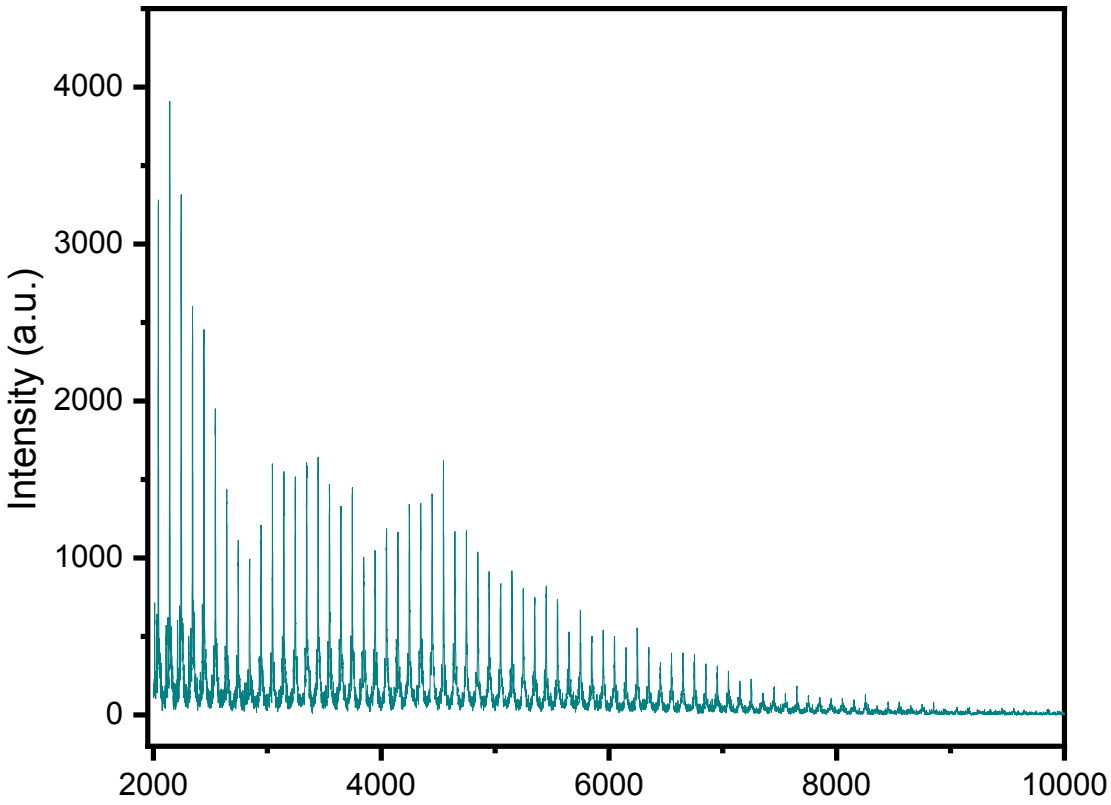

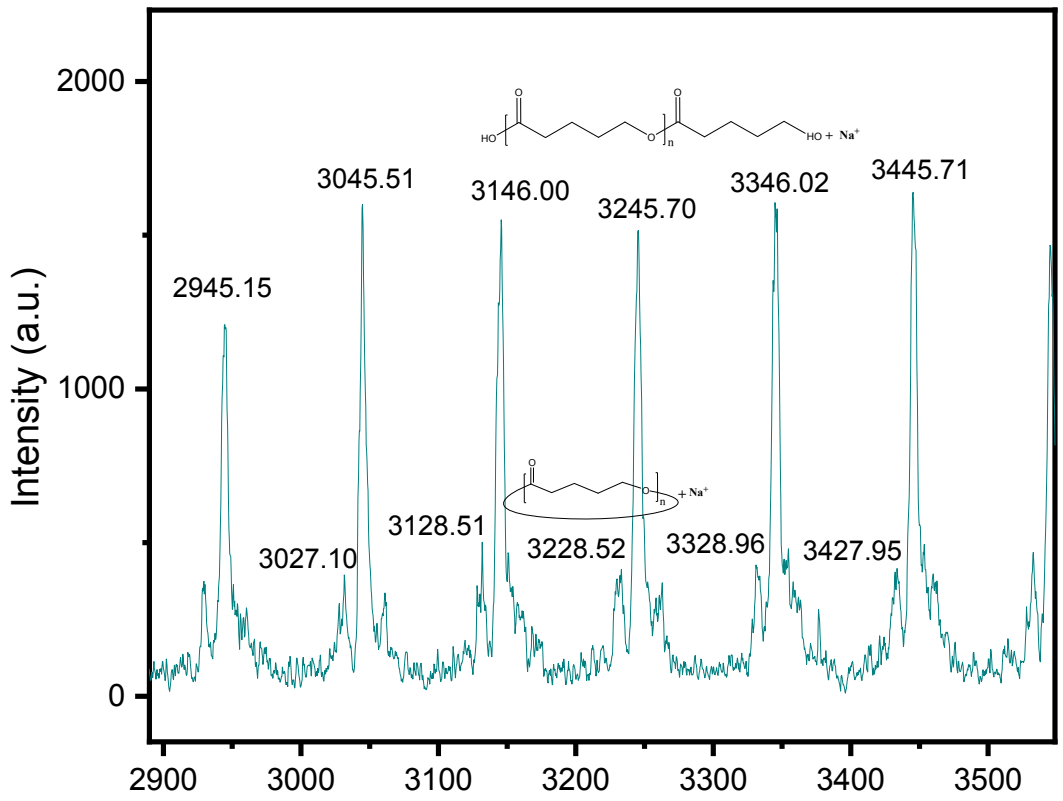

Figure S7. Mass spectrum of PVL by using **7** in the absence of BnOH (run 11, Table S2).

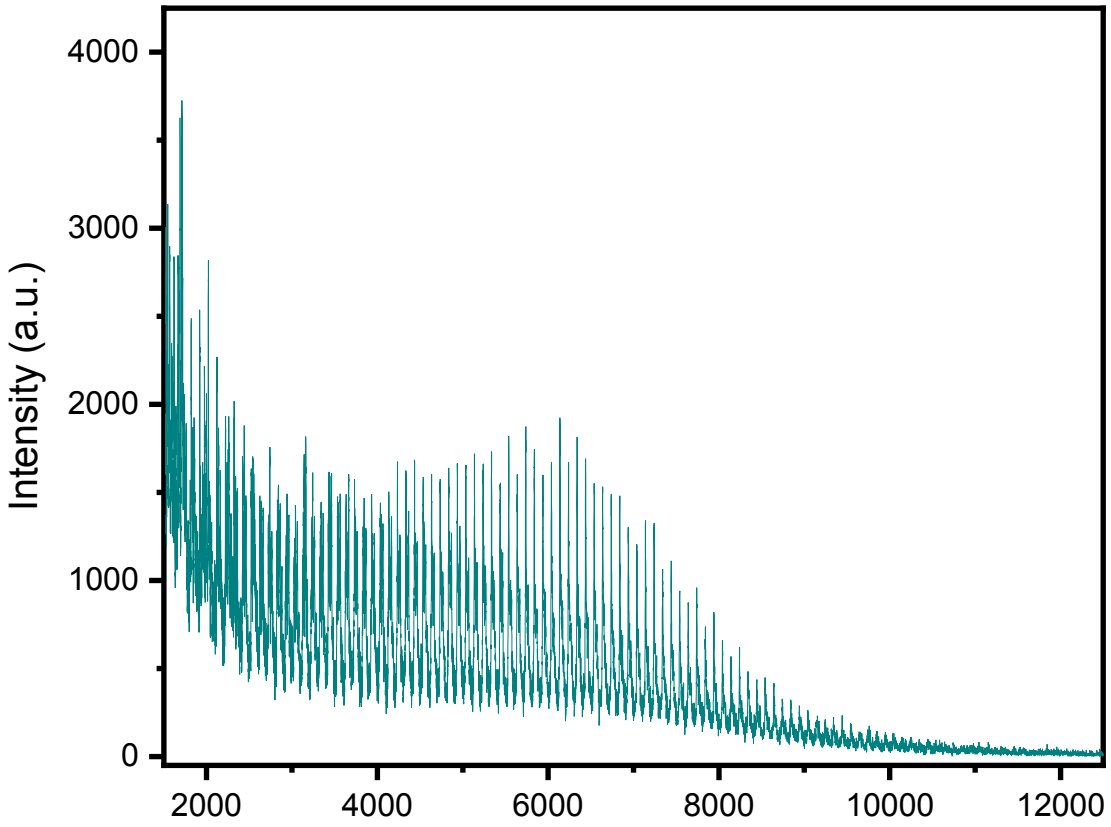

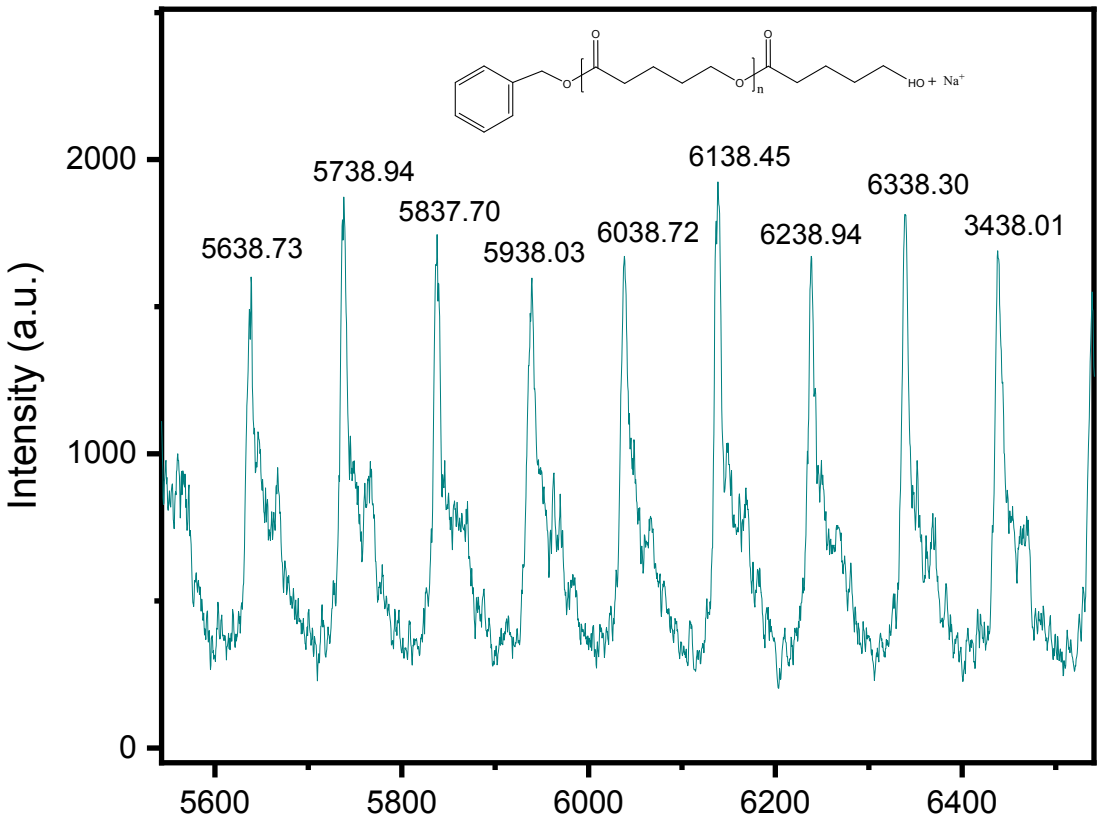

Figure S8. Mass spectrum of PVL by using **7**/BnOH (run 12, Table 3). [M = 108.05 (BnOH) + n × 100.12 (VL) + 22.99 (Na^+)].

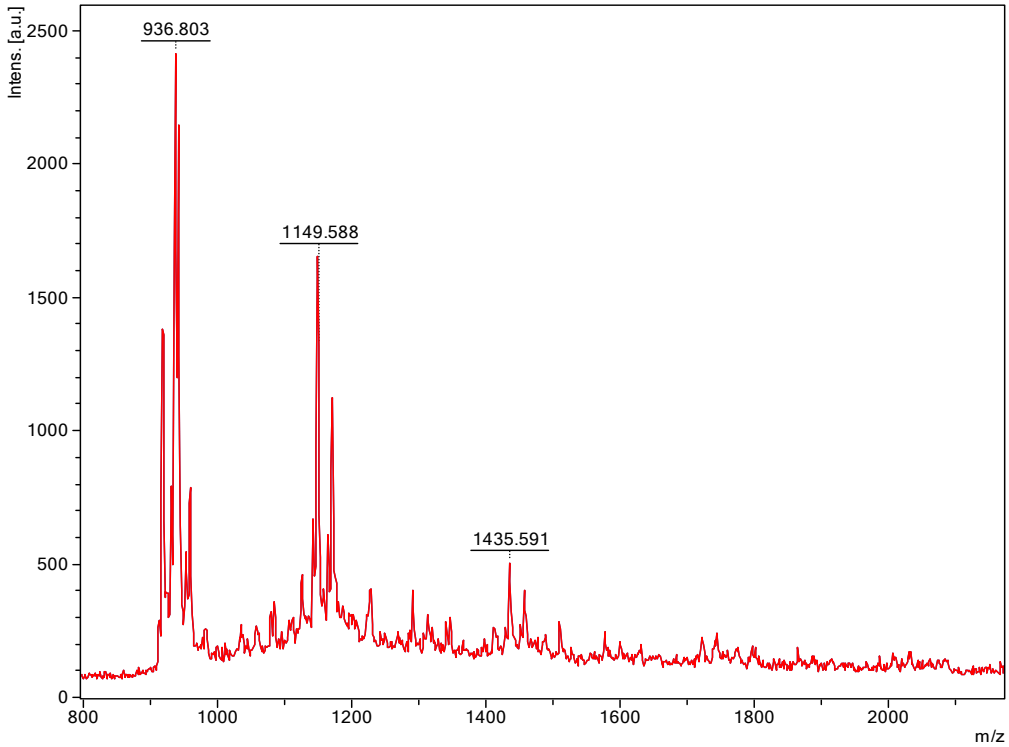

Figure S9. Mass spectrum of co-polymer (ε-CL +δ-VL) by using **I** in the absence of BnOH (run 14, Table 4).

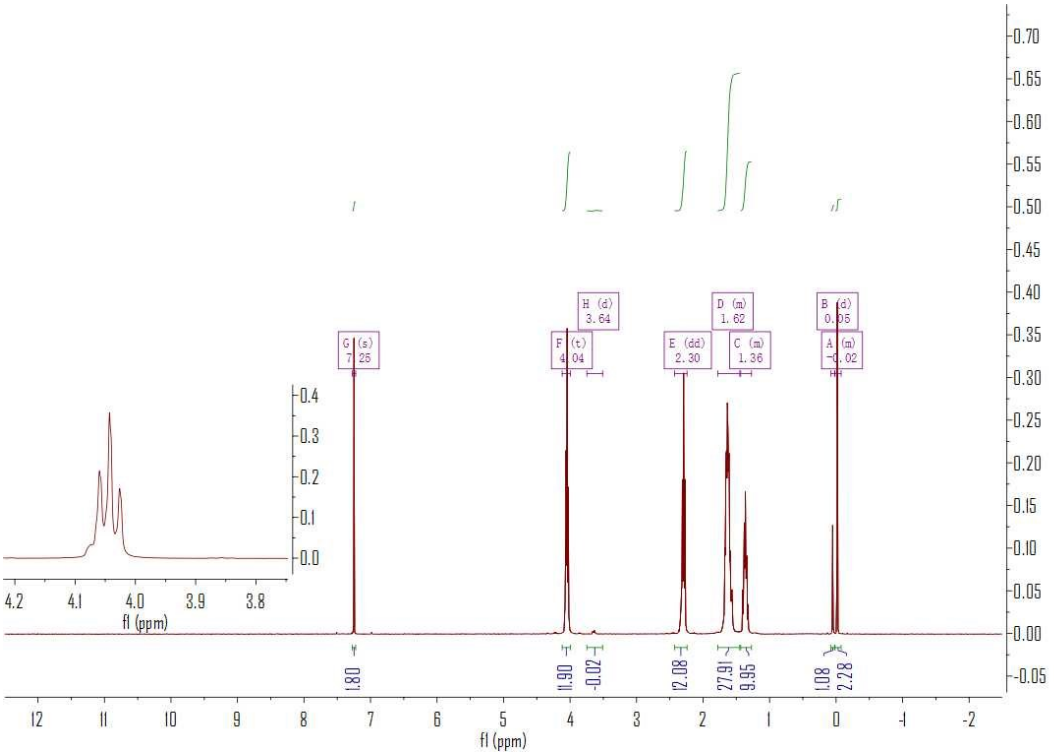

Figure S10. ^{1}H NMR spectrum ($CDCl_3$, 400 MHz, 298 K) of the PCL synthesized with **6** in the absence of BnOH (run 10, Table S1).

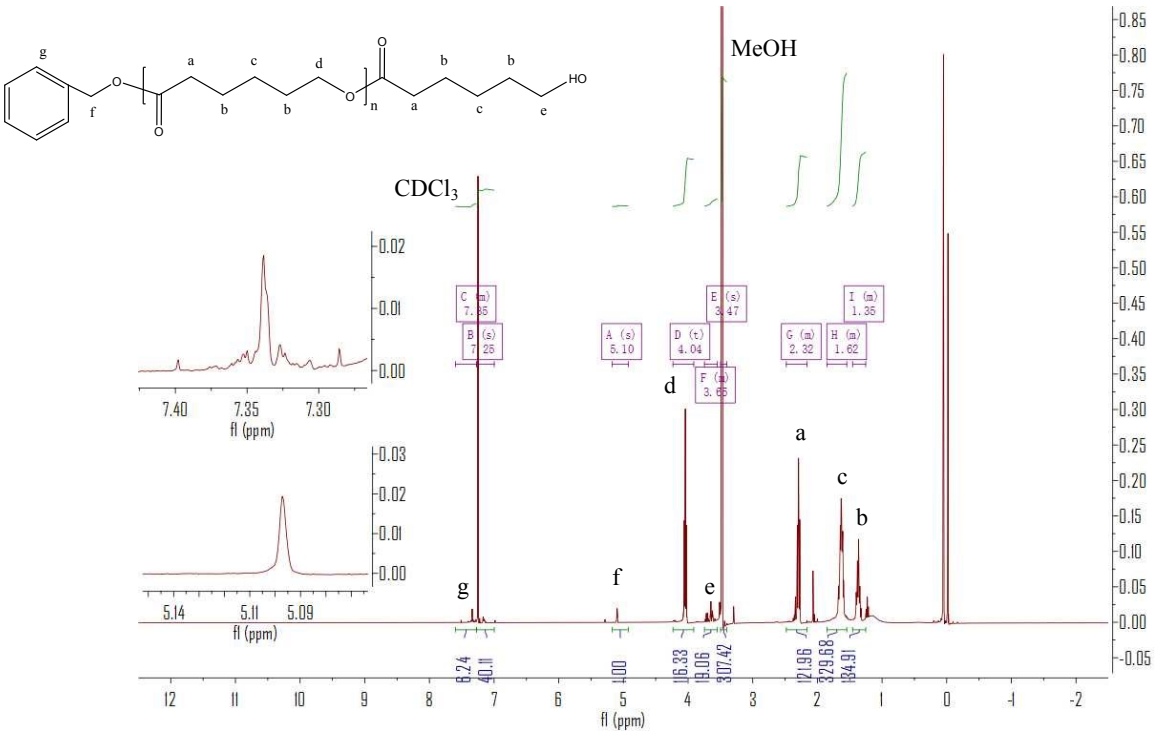

Figure S11. ^{1}H NMR spectrum ($CDCl_3$, 400 MHz, 298 K) of the PCL synthesized with **6**/BnOH (run 11, Table 2).

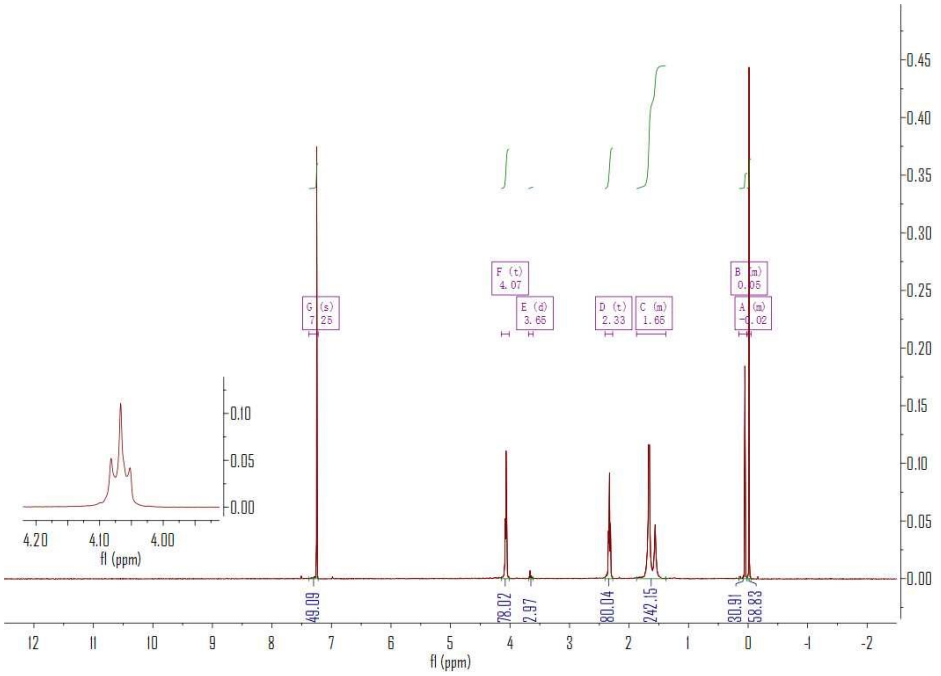

Figure S12. ^{1}H NMR spectrum ($CDCl_3$, 400 MHz, 298 K) of the PVL synthesized with **8** in the absence of BnOH (run 12, Table S2).

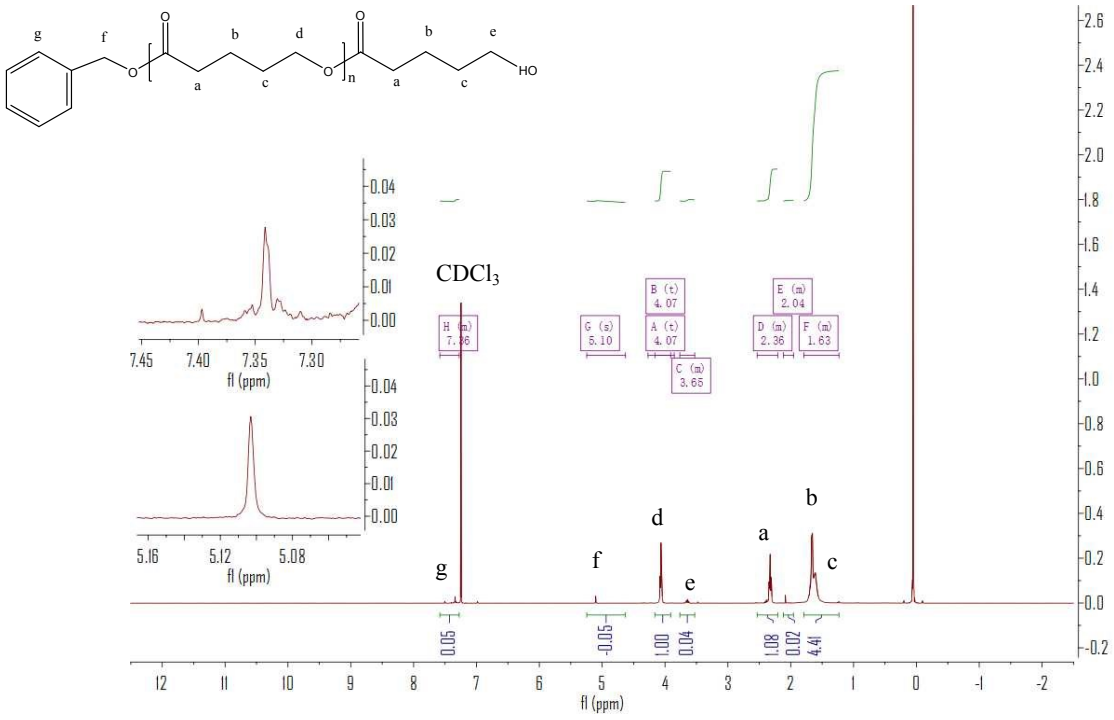

Figure S13. ^{1}H NMR spectrum ($CDCl_3$, 400 MHz, 298 K) of the PVL synthesized with **1**/BnOH (run 1, Table 3).

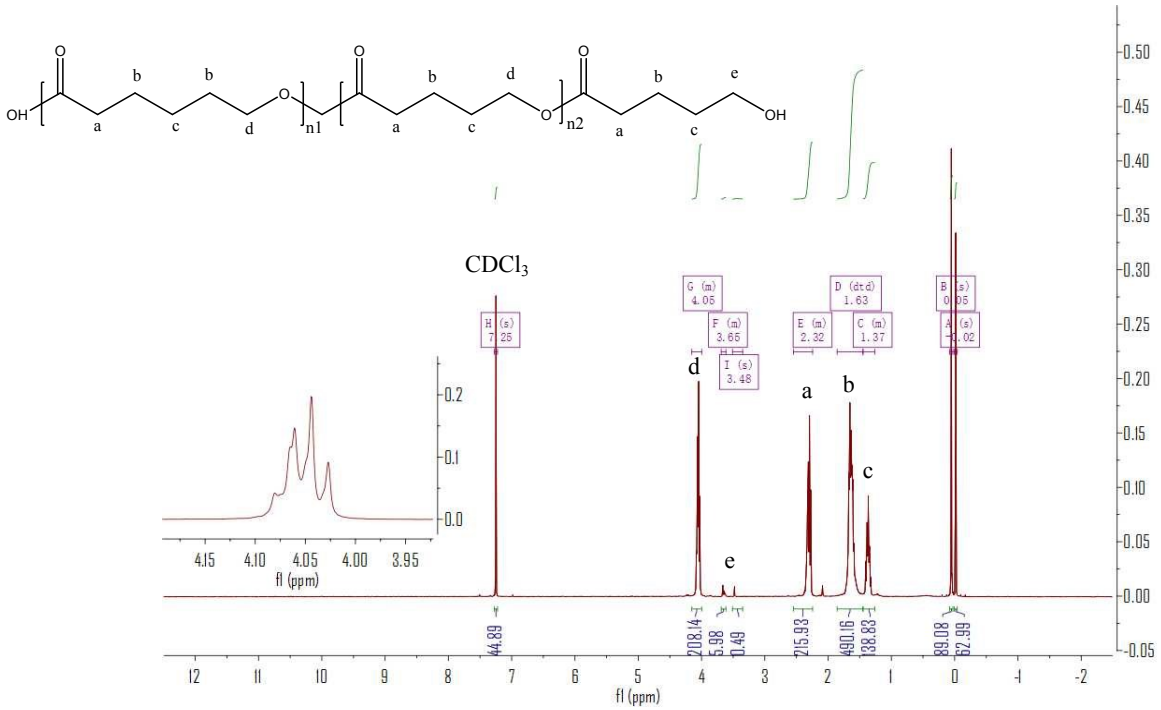

Figure S14. ^{1}H NMR spectrum ($CDCl_3$, 400 MHz, 298 K) of the CL-VL Copolymer (1:1 ratio CL/VL) synthesized with **I** in the absence of BnOH. (run 15, Table 4).

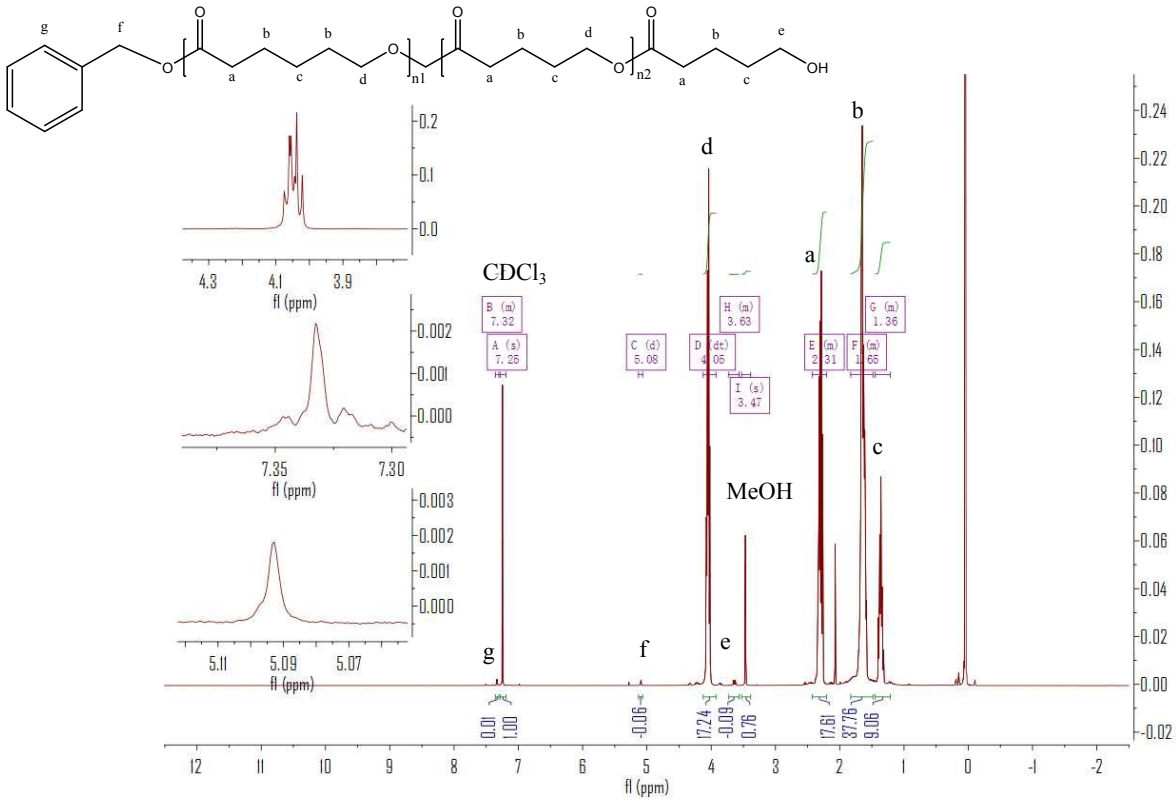

Figure S15. ^{1}H NMR spectrum ($CDCl_3$, 400 MHz, 298 K) of the CL-VL Copolymer (1:1 ratio CL/VL) synthesized with **1**/BnOH. (run 1, Table 4).

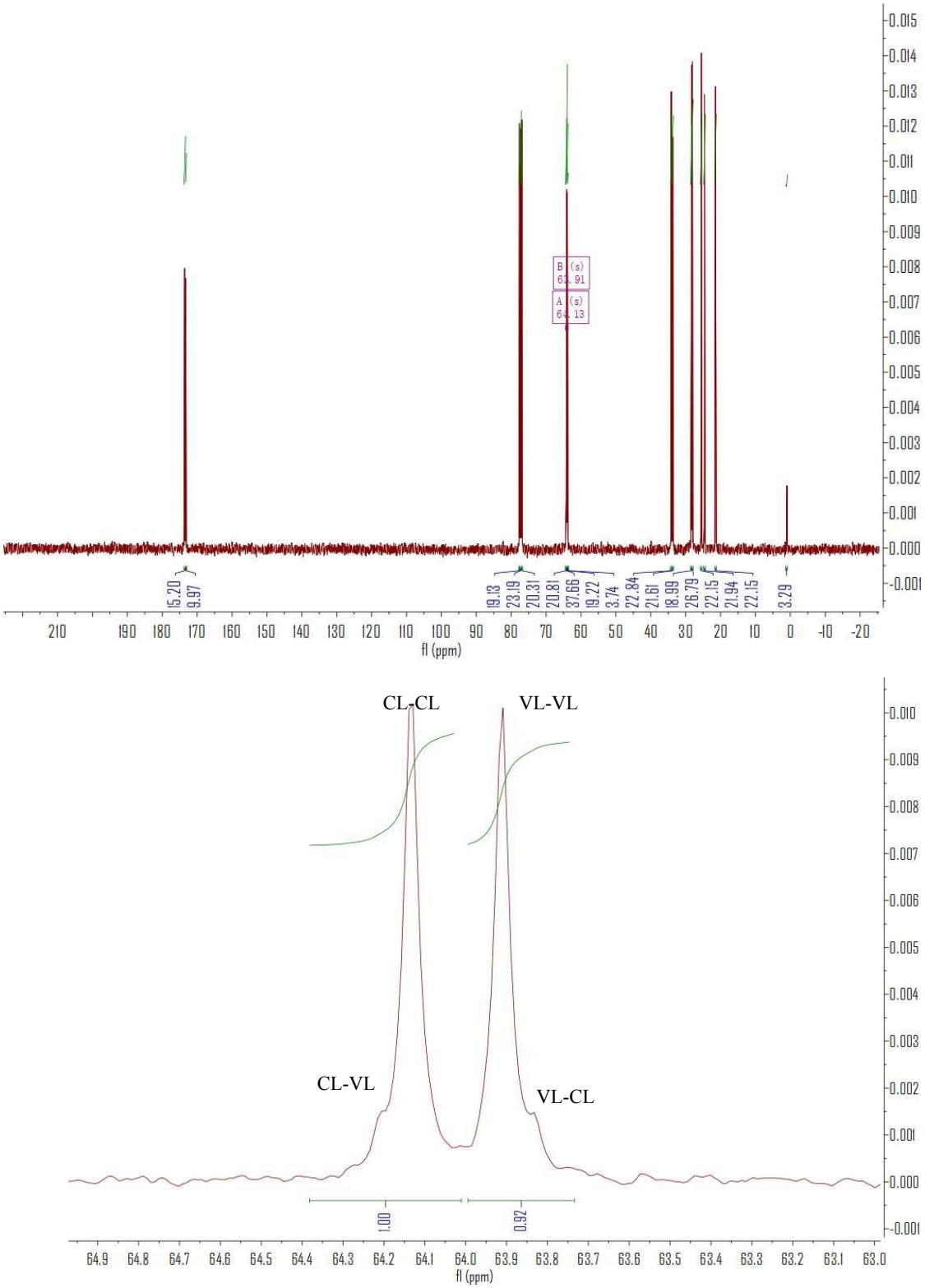

Figure S16. ^{13}C NMR spectrum ($CDCl_3$, 400 MHz, 298 K) of the CL-VL Copolymer (run 1, Table 4)

Equation S1. Determination of number-average sequence length for CL[1]

$$L_{CL}=[(I_{CL-CL})/(I_{VL-CL})]+1$$

Where I_{CL-CL} and I_{VL-CL} is the area of the peak belonging to the CL-CL and VL-VL dyad, respectively.

Equation S2. Determination of number-average sequence length for VL. [1]

$$L_{VL}=[(I_{VL-VL})/(I_{CL-VL})]+1$$

Where I_{VL-VL} and I_{CL-VL} is the area of the peak belonging to the VL-VL and CL-VL dyad, respectively.

Equation S3. Determination of the Randomness Character (R). [1]

$$R=1/(L_{CL}) + 1/(L_{VL})$$

Completely block Copolymers: R = 0
Copolymers with a "blocking" tendency: R < 1
Completely random copolymers: R = 1
Copolymers with an alternating tendency: R >1
Completely alternating copolymers: R = 2

Complex characterization

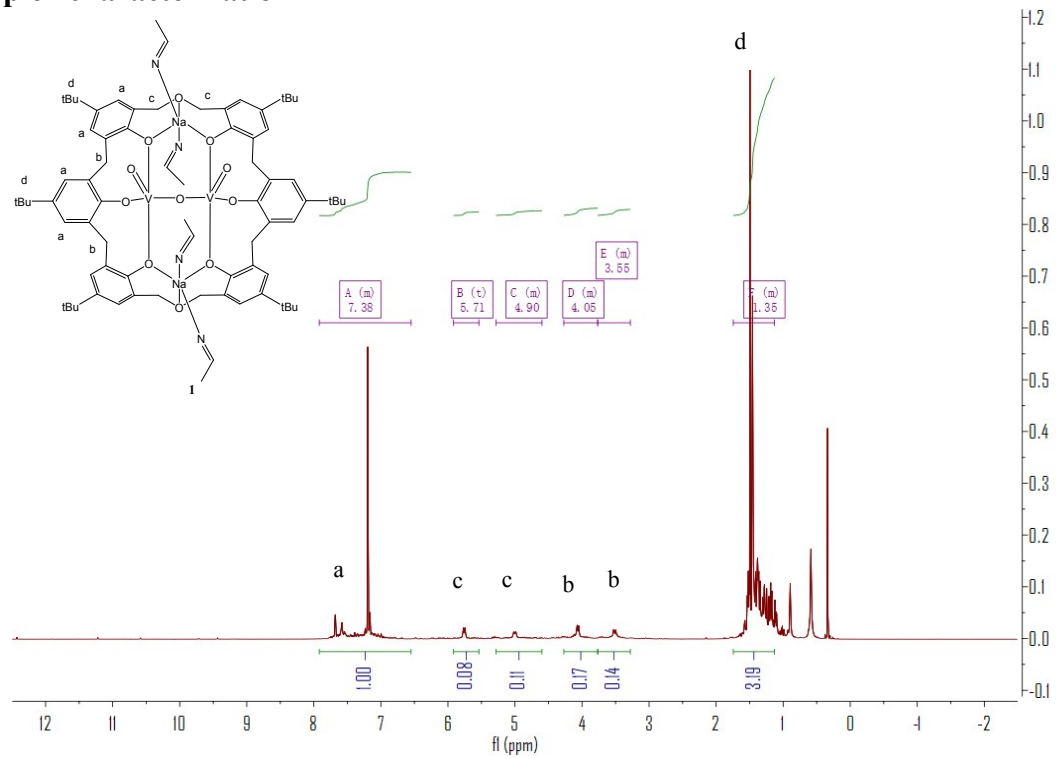

Figure S17. ^{1}H NMR ($CDCl_3$) results of complex **1**, ^{1}H NMR ($CDCl_3$) δ: 8.00-7.5 (m, 12H, aryl*H*), 5.71 (d, J=8.1, 4H, -OCH_2), 4.90 (d, J=8.1, 4H, OCH_2), 4.05 (d, J=8.0, 4H, -CH_2-), 3.53 (d, J=8.0, 4H, -CH_2), 2.05 (s, CH_3CN), 1.35-1.24 (m, 54H, C(CH_3)$_3$).

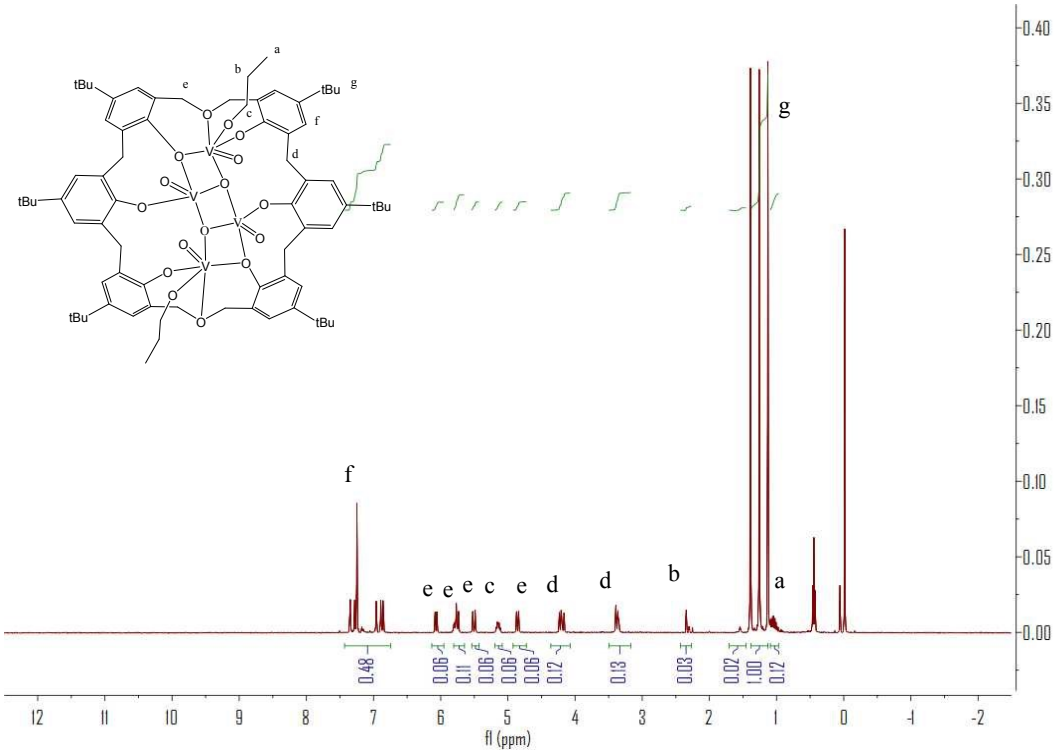

Figure S18. ^{1}H NMR ($CDCl_3$) results of complex **2**, ^{1}H NMR ($CDCl_3$) δ: 6.88-7.35 (m, 12H, aryl*H*), 6.07 (d, J=4.8 Hz, 2H, -OCH_2-), 5.77 (m, 2H, -OCH_2-), 5.51 (d, J=4.8 Hz, 2H, -OCH_2-) 5.15 (m, 2H, -OCH_2CH$_2$CH$_3$), 4.86 (d, J=4.8 Hz, 2H, -OCH_2-), 4.20 (m, 4H, -CH_2-), 3.40 (d, J=12.4 Hz, 4H, -CH_2-), 2.32 (m, 4H, -OCH$_2$CH_2CH$_3$), 1.13-1.49 (m, 54H, C(CH_3)$_3$), 1.02 (m, 6H, -OCH$_2$CH$_2$CH_3).

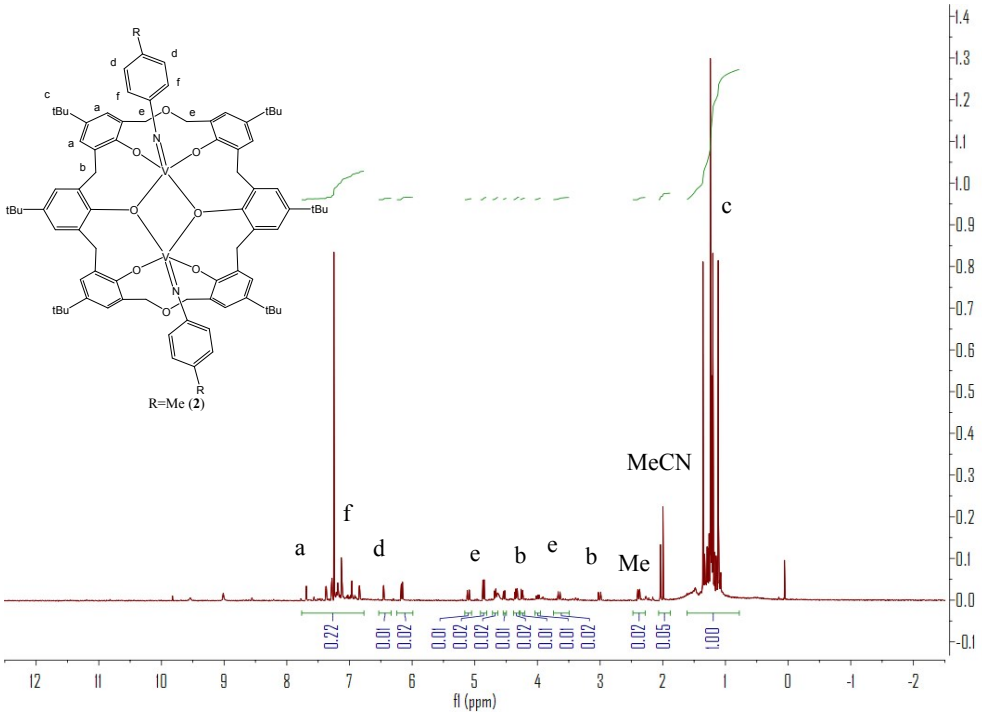

Figure S19. ^{1}H NMR ($CDCl_3$) results of complex **3**, ^{1}H NMR ($CDCl_3$) δ: 7.78–6.85 (m, 12H, aryl-*H*), 6.46 (d, J=8.4 Hz, 4H , N-C$_6H_4$-), 6.16 (d, J=8.4 Hz, 4H, -N-C$_6H_4$-), 4.86-5.10 (d, J=7.6 Hz, 4H, OCH_2-), 4.53-4.66 (m, 4H, -OCH_2-), 4.34-4.25 (m, 4H, -CH_2) 3.66-4.00 (d, J=12.4 Hz, 4H, -CH_2), 2.35 (m, 6H, *p*-tolyl-CH_3), 2.05 (s, 3H, MeCN) 1.49 (m, 54H, C(CH_3)$_3$).

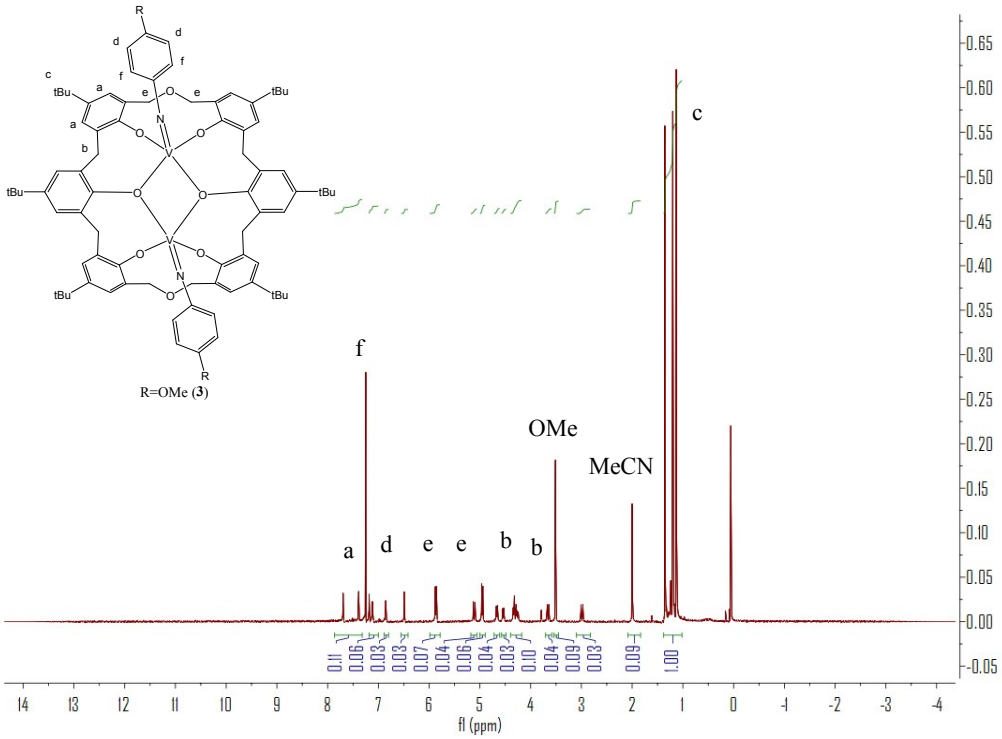

Figure S20. ^{1}H NMR ($CDCl_3$) results of complex **4**, ^{1}H NMR ($CDCl_3$) δ: 6.87-7.54 (m, 12H, aryl*H*), 6.49 (d, J=8.0 Hz, 4H, -NC_6H_4-OMe), 5.88 (d, J=8.0 Hz, 4H, -NC_6H_4-OMe), 5.11 (d, J=6.8 Hz, 4H, -OCH_2-), 4.95 (d, J=6.8 Hz, 4H, -OCH_2-), 4.47-4.67 (m, 4H, -CH_2-) ,3.64 (d, J=5.2 Hz, 4H, -CH_2-), 3.51 (s, 6H, *p*-C_6H_4-OCH_3), 2.01 (s, 3H, MeCN), 1.35-1.15 (m, 54H, $C(CH_3)_3$).

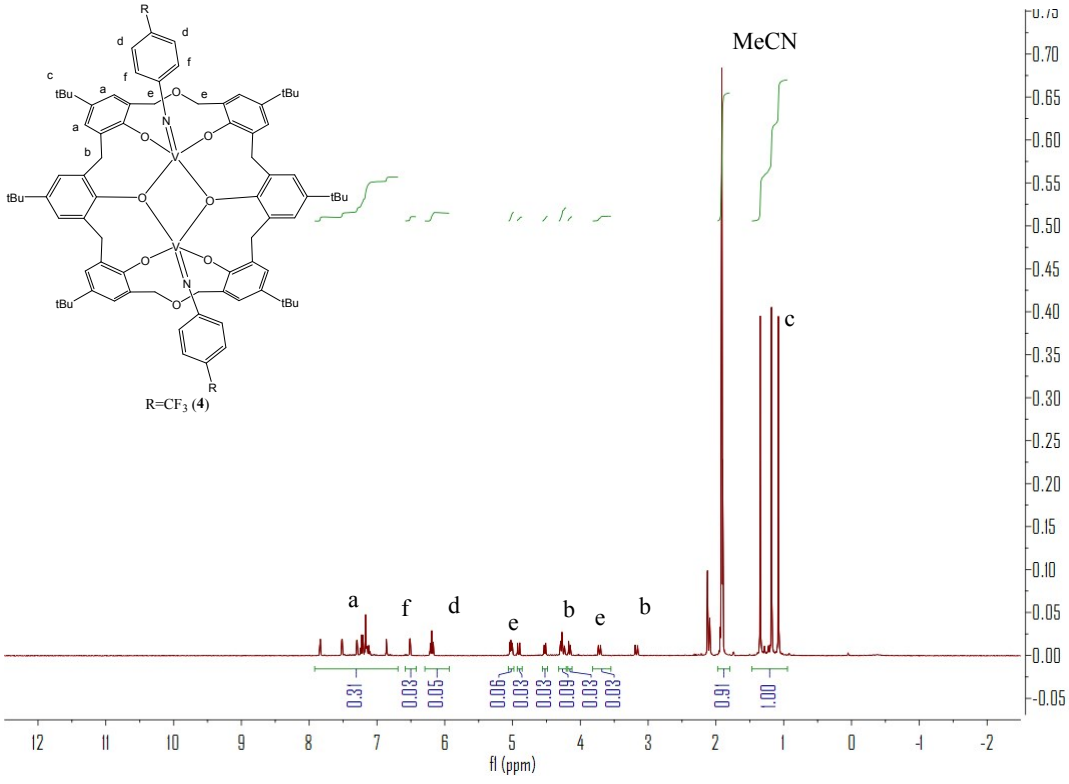

Figure S21. ^{1}H NMR ($CDCl_3$) results of complex **5**. ^{1}H NMR ($CDCl_3$) δ: 6.84-7.82 (m, 12H, aryl*H*), 6.51 (d, J=8.8, 4H, -C_6H_4- CF_3), 6.19 (m, 4H, -C_6H_4-CF_3), 5.02-4.91 (m, 4H, -OCH_2-), 4.52 (d, J=5.2, 4H, -OCH_2-), 4.27-4.16 (m, 4H, -CH_2-) ,3.72 (m , 4H, -CH_2-), 1.95 (s, 3H, MeCN), 1.35-1.06 (m, 54H, $C(CH_3)_3$).

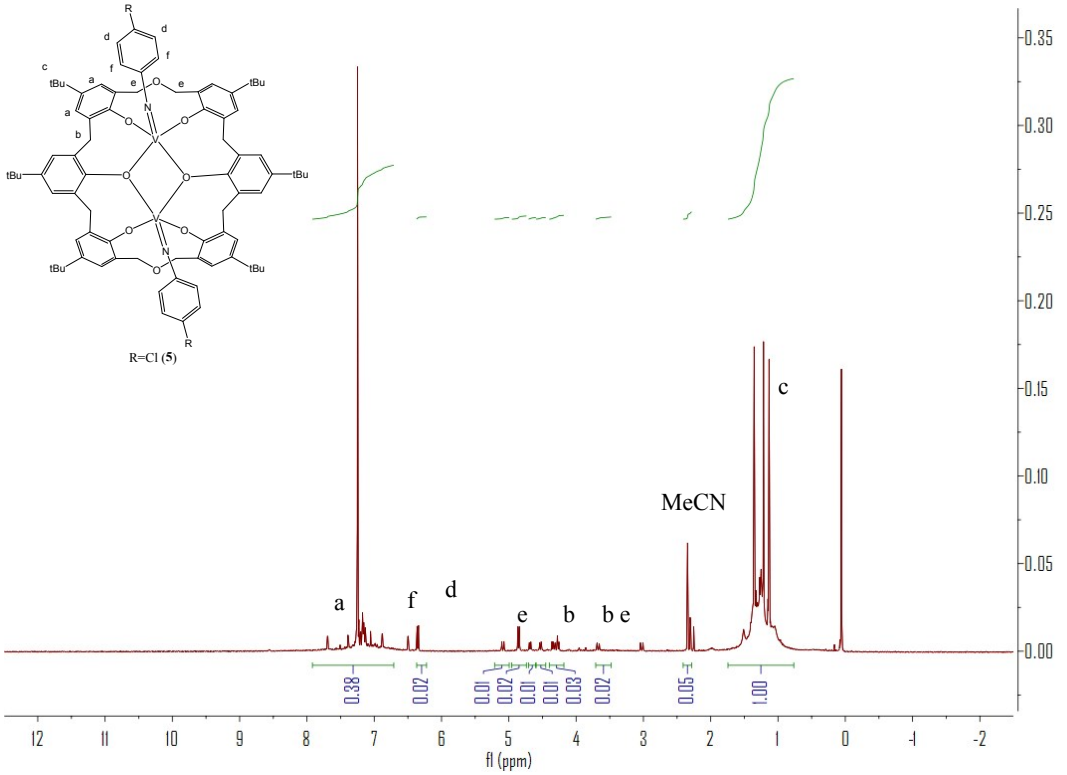

Figure S22. ^{1}H NMR ($CDCl_3$) results of complex **6**, ^{1}H NMR ($CDCl_3$) δ: 6.88-7.69 (m, 12H, aryl*H*), 6.50 (d, J=10.0 Hz, 4H, -C_6H_4-Cl), 6.35 (d, J=10.0, 4H, -C_6H_4-Cl), 4.86-5.09 (m, J=10.0 Hz, 4H, -OCH_2-), 4.68 (d, J=10.0 Hz, 4H, -OCH_2-), 4.31-4.53 (m, 4H, -CH_2-) ,3.67 (d, J=12.8 Hz, 4H, -CH_2-), 1.13-1.35 (m, 54H, C(CH_3)$_3$).

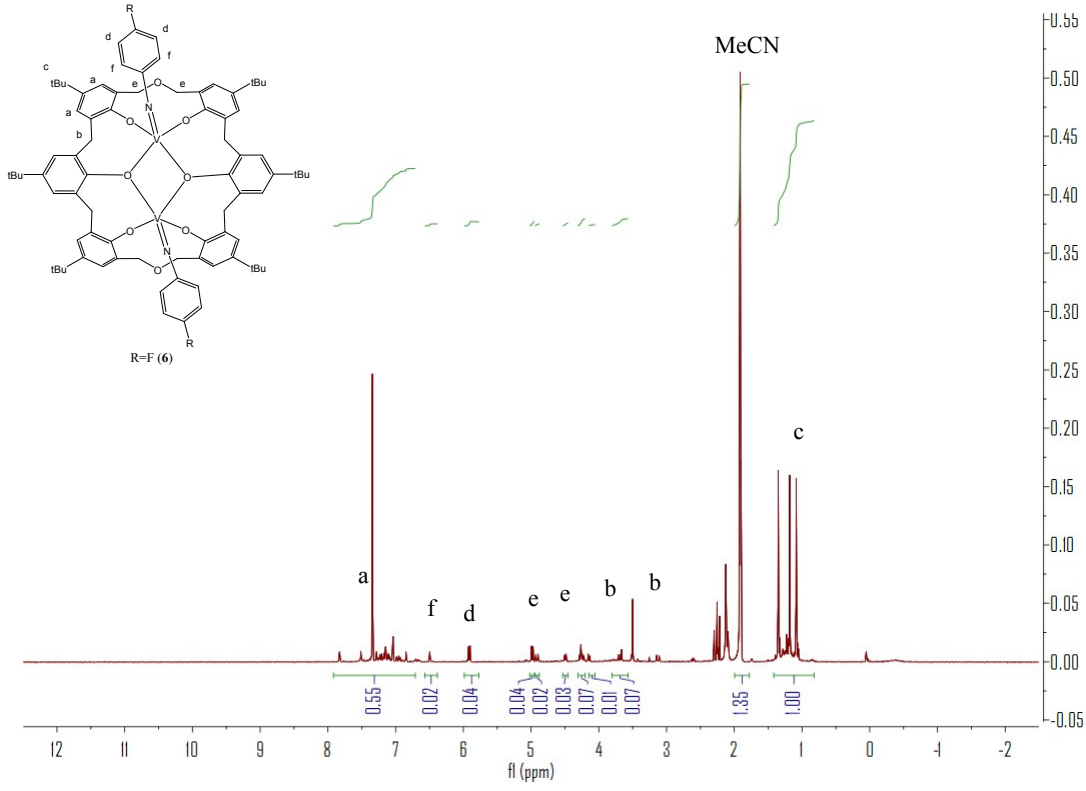

Figure S23. ^{1}H NMR ($CDCl_3$) results of complex **7**, ^{1}H NMR ($CDCl_3$) δ: 6.84-7.81 (m, 12H, aryl*H*), 6.49 (d, J=6.8 Hz, 4H, -NC_6H_4-F), 5.91 (d, J=6.8 Hz, 4H, -NC_6H_4-F), 4.91-4.98 (d, J=8.8 Hz, 4H, -OCH_2-), 4.49 (d, J=8.8 Hz, 4H, -OCH_2-), 4.13-4.26 (m, 4H, -CH_2-), 3.69 (d, J=5.2 Hz, 4H, -CH_2-), 1.36-1.09 (m, 54H, C(CH_3)$_3$).

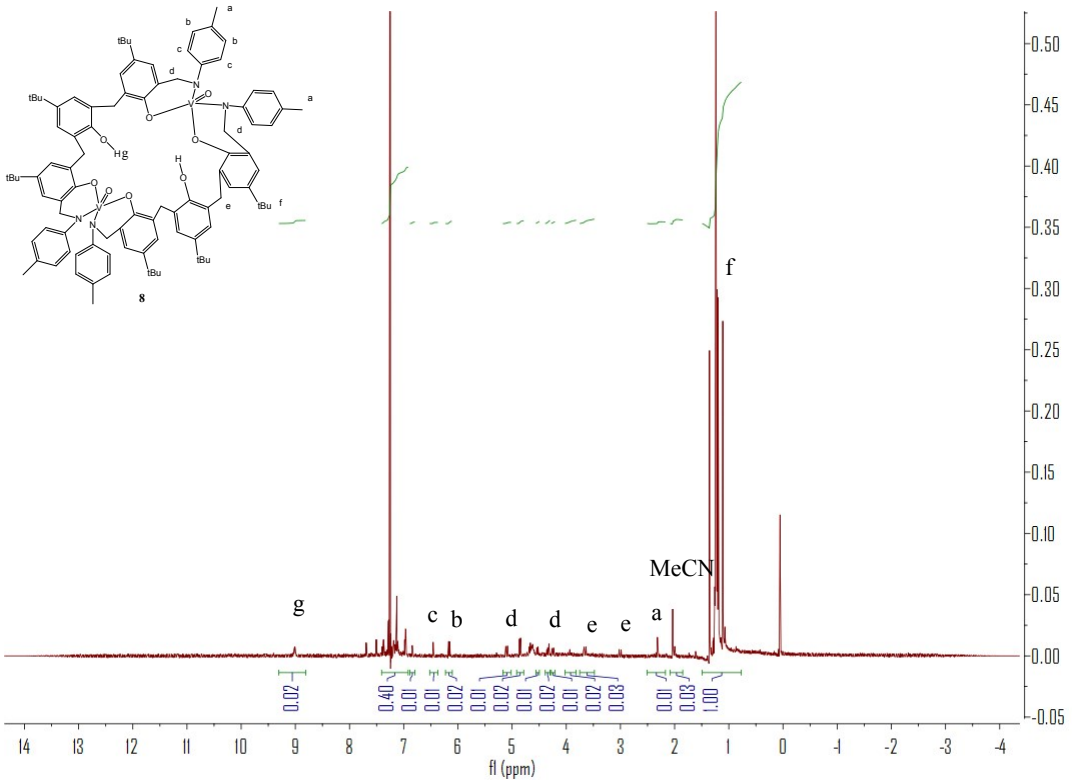

Figure S24. ^{1}H NMR ($CDCl_3$) results of complex **8**, ^{1}H NMR ($CDCl_3$) δ: 9.01 (s, 2H, -OH), 6.84-7.68 (m, 12H, aryl*H*), 6.45 (d, J=8.4 Hz, 4H, -NC_6H_4-Me), 6.16 (d, J=8.4 Hz, 4H, -NC_6H_4-Me), 4.85-5.10 (d, J=9.6 Hz, 4H, -N-CH_2-), 4.53-4.65 (d, J=9.6 Hz, 4H, -N-CH_2-), 4.25-4.34 (m, 4H, -CH_2-), 3.65 (d, J=12.8 Hz, 4H, -CH_2-), 2.33 (m, 12H, -CH_3), 2.01 (s, 3H, MeCN), 1.11-1.36 (m, 54H, C(CH_3)$_3$).

Polyethylene spectra

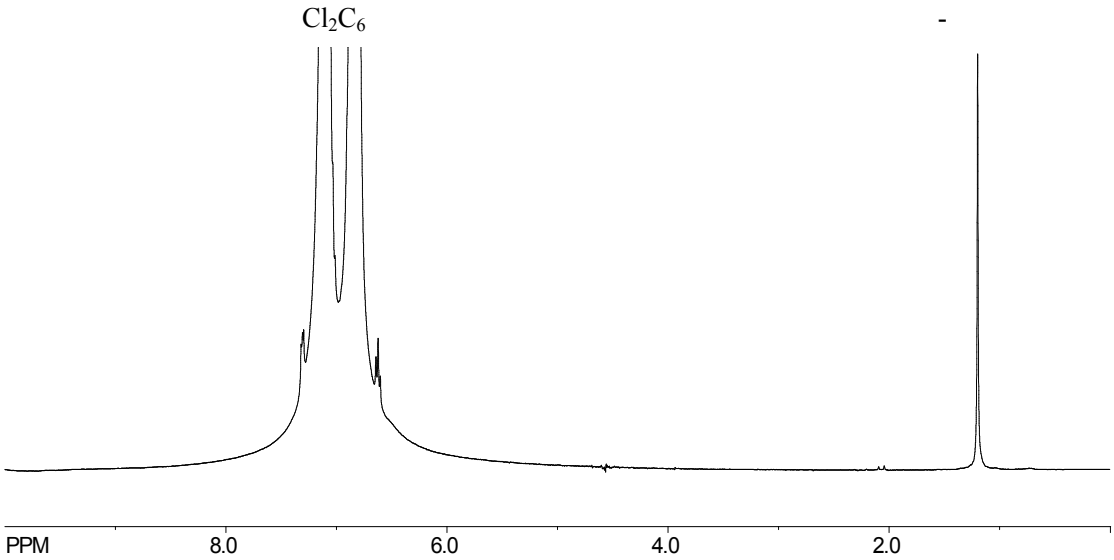

Figure S25. ^{1}H NMR spectrum ($Cl_2C_6H_4$, 100 °C) of polyethylene (run 6, Table 5).

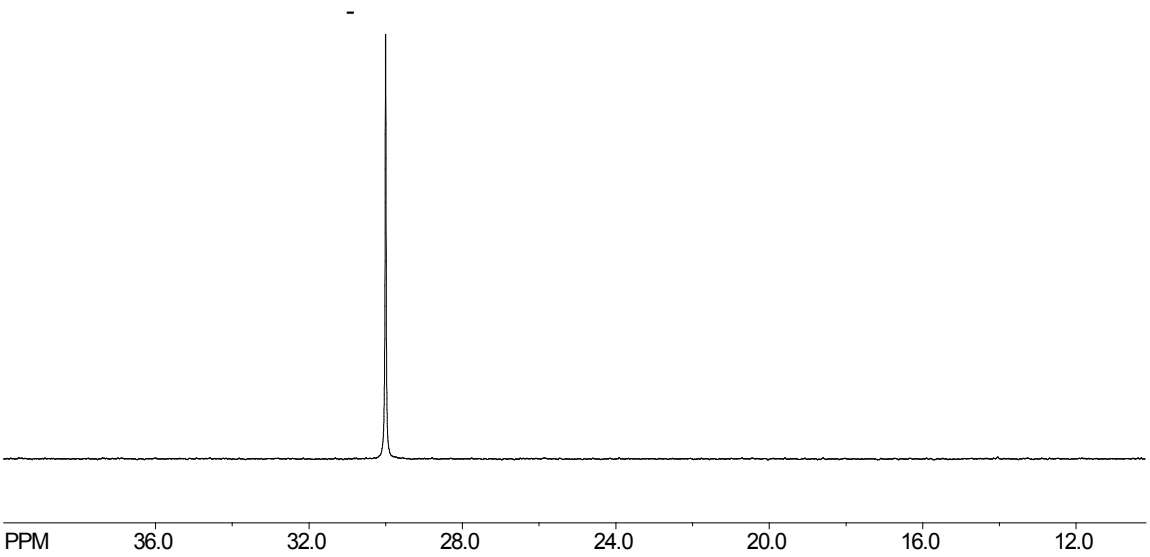

Figure S26. ^{13}C NMR spectrum ($Cl_2C_6H_4$, 100 °C) of polyethylene (run 6, Table 5).

References

[1] (a) Q. Hu, S.-Y. Jie, P. Braunstein and B.-G. Lia, *Chinese J. Polym. Sci*. 2020, **38**, 240–247; (b) M. A. Woodruff and D. W. Hutmacher, *Prog. Polym. Sci.,* 2010, **35**, 1217−1256; (c) T. Wu, Z. Wei, Y. Ren, Y. Yu, X. Leng and Y. Li, *Polym. Degrad. Stab.,* 2018, **155**, 173−182; (d) M. T. Hunley, N. Sari, and K. L. Beers, *ACS Macro Lett*., 2013, **2**, 375−379. (e) Z. Sun, Y. Zhao, O. Santoro, M. R. J. Elsegood, E. V. Bedwell, K. Zahra, A. Walton, and C. Redshaw, *Catal. Sci. Technol.*, 2020, **10**, 1619−1639.